

Exact solutions and critical chaos in dilaton gravity with a boundary

Maxim Fitkevich^{a,b} Dmitry Levkov^a Yegor Zenkevich^{1c,d,e}

^a*Institute for Nuclear Research of the Russian Academy of Sciences, 60th October Anniversary Prospect 7a, Moscow 117312, Russia*

^b*Moscow Institute of Physics and Technology, Institutskii per. 9, Dolgoprudny 141700, Moscow Region, Russia*

^c*Dipartimento di Fisica, Università di Milano-Bicocca, Piazza della Scienza 3, I-20126 Milano, Italy*

^d*INFN, sezione di Milano-Bicocca, I-20126 Milano, Italy*

^e*National Research Nuclear University MEPhI, Moscow 115409, Russia*

E-mail: fitkevich@phystech.edu, levkov@ms2.inr.ac.ru,
yegor.zenkevich@gmail.com

ABSTRACT: We consider the model of $(1 + 1)$ -dimensional dilaton gravity with a reflecting dynamical boundary. The boundary cuts off the region of strong coupling and makes the model causally similar to the multidimensional spherically-symmetric gravity. We demonstrate that this model is exactly solvable at the classical level and possesses an on-shell $SL(2, \mathbb{R})$ symmetry. After introducing general classical solution of the model, we study in detail a large class of particular solutions describing reflection of matter waves off the boundary at low energies and formation of black holes at energies above critical. Such solutions can be related to the eigenstates of the auxiliary integrable system, the Gaudin spin chain. We argue that despite being exactly solvable, the model in the critical regime, i.e. at the verge of black hole formation, displays dynamical instabilities specific to chaotic systems. We believe that this model will be useful for studying black holes and gravitational scattering.

¹On leave of absence from ITEP, Moscow 117218, Russia

Contents

1	Introduction	1
2	The model	4
2.1	Adding the boundary	4
2.2	Solution in the bulk and reflection laws	5
2.3	Simple equation for the boundary	7
2.4	On-shell conformal symmetry	10
3	Integrable sector	11
3.1	General solution	11
3.2	Soliton solutions with power-law singularities	12
3.3	Simplifying the coefficient equations	15
3.4	$SL(2, \mathbb{C})$ symmetry	15
3.5	Relation to the Gaudin model	16
3.6	Positivity condition	19
4	Critical chaos	20
4.1	Perturbative expansion in the critical regime	20
4.2	Thunderpop instability	22
5	Discussion	24
A	Field equations and boundary conditions	25
A.1	Derivation	25
A.2	Solution in the conformal gauge	26
B	Bethe Ansatz for the Gaudin model	27

1 Introduction

The models of two-dimensional dilaton gravity were popular for decades [1–3]. Some of them describe spherically-symmetric sectors of multidimensional gravities with the dilaton fields ϕ related to the sizes of the extra spheres¹. Some others are exactly solvable at the semiclassical [4, 5] or quantum [3] levels which makes them valuable for studying black holes and gravitational scattering [6–8].

¹In particular, gravitational sector of the CGHS model [4] can be obtained by spherical reduction of D -dimensional gravity at $D \rightarrow +\infty$ [3].

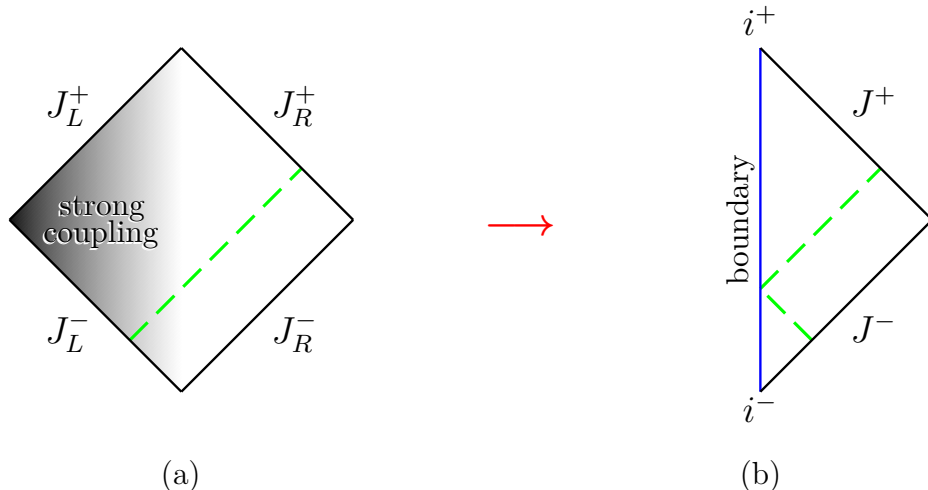


Figure 1. Penrose diagrams of Minkowski vacuum in (a) the original CGHS model and (b) the model with a boundary. The dashed lines are light rays extending from J^- to J^+ .

These models become particularly important in the context of information paradox [9, 10] confronting apparent loss of quantum coherence during black hole evaporation with the principles of quantum theory. Since unitarity of quantum gravity is strongly supported by the AdS/CFT correspondence [11, 12], modern AMPS argument [13, 14] suggests dramatic violation of the equivalence principle (“firewalls”) in the vicinity of old black hole horizons, see [15, 16] for earlier works. This feature, if exists, may leave “echoes” in the gravitational wave signal [17, 18] to be detected by LIGO [19, 20]. From the theoretical viewpoint, further progress can be achieved by understanding unitary evolution of black holes outside of the explicit AdS/CFT framework. This brings us to the arena of two-dimensional models which may, in addition, clarify relation of black holes to quantum chaos [21–26], cf. [27] or to the BMS-like symmetries [28, 29].

Unfortunately, solvable models of dilaton gravity in two dimensions essentially differ from their multidimensional cousins. Consider e.g. the celebrated Callan-Giddings-Harvey-Strominger (CGHS) model [4], see [1, 2] for reviews. Its two-dimensional Minkowski vacuum in Fig. 1a, unlike the multidimensional vacua, has disconnected sets of “left” and “right” infinities J_L^\pm , J_R^\pm , and transitions between those are expected [30] to be important for the information loss problem. Besides, the CGHS model is strongly coupled [31] near the “left” infinities which puts its semiclassical results on shaky ground. It was recently suggested [32] that due to the above peculiarities evaporation of the CGHS black holes leads to remnants rather than firewalls.

We consider non-minimal model of dilaton gravity proposed² in [33, 34], see also [31, 38–41]. The region of strong coupling in this model is cut off by the reflective

²Similar models appeared recently in the context of near AdS_2 / near CFT_1 holography [35–37].

dynamical boundary placed at a fixed value $\phi = \phi_0$ of the dilaton field, see Fig. 1b. Parameter $e^{2\phi_0} \ll 1$ plays the role of a small coupling constant. We explicitly obtain the reparametrization-invariant action of this model by restricting the classical CGHS action to the space-time region $\phi < \phi_0$ and adding the appropriate boundary terms. Note that the original CGHS model is formally restored in the limit $\phi_0 \rightarrow +\infty$ which shifts the regulating boundary in Fig. 1b all the way the left. We do not consider this limit avoiding potential problems with strong coupling, cf. [42–44].

As an additional bonus, the model with a boundary is causally similar to spherically-symmetric multidimensional gravity, cf. Fig. 1b. The price to pay, however, is nonlinear equation of motion for the boundary which, if non-integrable, may damage major attractive property of the CGHS model — its solvability. Note that the previous studies of this or similar models were relying on numerical [39–41, 45] or shock-wave [33, 34, 38] solutions.

In this paper we demonstrate that the classical CGHS model with a boundary is exactly solvable. We obtain general solution of the classical equations and construct an infinite number of particular soliton solutions. The latter describe reflection of matter waves off the boundary at low energies and formation of black holes at energies above some critical values, see Figs. 2a and c. Each solution is characterized by N integers or half-integers s_1, \dots, s_{2N} , the same number of complex parameters, and finite-range ordinal number r . The parameters of the solitons satisfy inequalities due to positivity of energy.

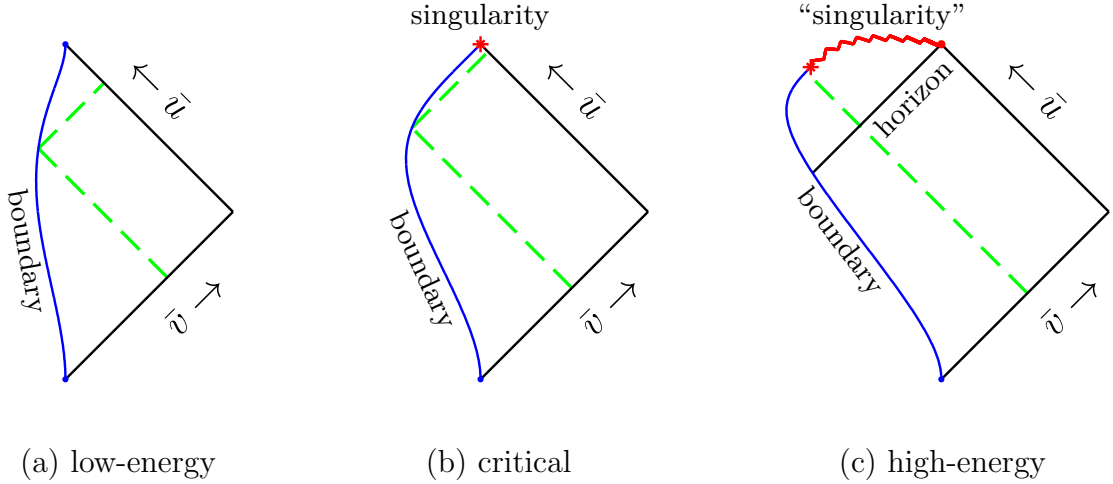


Figure 2. The simplest exact solution ($s_1 = s_2 = 1$) in the model with a boundary at different values of parameters. Finite-range light-cone coordinates (\bar{u}, \bar{v}) are used. The centers of the incoming and reflected matter wave packets are marked by the dashed lines.

We establish one-to-one correspondence between the above solitons and the eigenstates of the auxiliary integrable system — the rational Gaudin model [46–48]. This allows one to classify these solutions and study their properties.

Surprisingly, we find that equation of motion for the boundary is invariant under conformal transformations $v \rightarrow w(v)$, where v is the light-cone coordinate, w is an arbitrary function. These transformations relate physically distinct solutions, and one should not confuse them, say, with the residual reparametrization symmetry of [38, 39]. In particular, the transformations from the global $\text{SL}(2, \mathbb{R})$ subgroup change massless matter field(s) f of the model as the standard zero-weight fields. They also map the solitons discussed above into other solutions of the same kind. The transformations with nonzero Schwarzian derivative act non-linearly on f , and we do not consider them in detail.

Finally, we study dynamics of the model in the critical regime, i.e. at the verge of black hole formation, cf. Fig. 2b. We demonstrate that in this limit scattering of matter waves off the boundary displays instabilities specific to chaotic systems: the final state of the process becomes extremely sensitive to the initial Cauchy data. This feature is in tune with the near-horizon chaos suggested in [23]. We argue that it impedes global integrability of the model, i.e. prevents one from choosing a complete set of smooth conserved quantities in the entire phase space.

In Sec. 2 we introduce dilaton gravity with a boundary and study its properties, in particular, equation for the boundary and its conformal symmetry. We construct exact solutions in Sec. 3. Critical chaos is considered in Sec. 4. In Sec. 5 we discuss possible applications of our results.

2 The model

2.1 Adding the boundary

We consider two-dimensional model with classical action

$$S = \int_{\phi < \phi_0} d^2x \sqrt{-g} [e^{-2\phi} (R + 4(\nabla\phi)^2 + 4\lambda^2) - (\nabla f)^2/2] \\ + e^{-2\phi_0} \int_{\phi=\phi_0} d\tau (2K + 4\lambda) , \quad (2.1)$$

where³ the integrand in the first line is the CGHS Lagrangian [4] describing interaction of the metric $g_{\mu\nu}$ and dilaton ϕ with massless scalar f ; the dimensionful parameter λ sets the energy scale of the model. In Eq. (2.1) we modified the CGHS action by restricting integration to the submanifold $\phi < \phi_0$ and adding the boundary terms at $\phi = \phi_0$. We introduced the proper time of the boundary τ , its extrinsic curvature $K = g^{\mu\nu} \nabla_\mu n_\nu$, and unit outer normal $n_\mu \propto \nabla_\mu \phi$.

In fact, the choice of the boundary action in Eq. (2.1) is limited. First, the Gibbons-Hawking term with extrinsic curvature is required for consistency of the

³We use $(-, +)$ signature and Greek indices $\mu, \nu, \dots = 0, 1$. We denote covariant derivatives by ∇_μ and Ricci scalar by R .

gravitational action [49]. Second, we assume no direct interaction of the matter field f with the boundary. Then the only possible generalization of our model would include an arbitrary constant in the last term of Eq. (2.1). However, this parameter needs to be fine-tuned in order to retain Minkowski solution (see below). Thus, Eq. (2.1) is the most general action describing interaction of the boundary with the gravitational sector of the CGHS model [33].

The quantity $e^{2\phi_0}$ is a coupling constant controlling loop expansion in our model. Indeed, after changing the variables to $\tilde{\phi} = \phi - \phi_0$ and $\tilde{f} = e^{\phi_0} f$ this parameter appears only in front of the classical action, $S = \tilde{S}/e^{2\phi_0}$, and therefore plays the role of a Planck constant. This makes our model classical at $e^{2\phi_0} \ll 1$.

It is clear that the bulk field equations in the model (2.1) are the same as in the original CGHS model [4][1, 2]. However, extremizing the action with respect to the boundary values of $g_{\mu\nu}$ and f , one also obtains reflective boundary conditions

$$n^\mu \nabla_\mu \phi = \lambda, \quad n^\mu \nabla_\mu f = 0 \quad \text{at} \quad \phi = \phi_0, \quad (2.2)$$

see Appendix A.1 for details. Note that the constant λ in the right-hand side of the first equation comes from the last term in Eq. (2.1). Besides, the second equation guarantees zero energy flux through the boundary.

Let us now recall [4] that linear dilaton vacuum

$$g_{\mu\nu} = \eta_{\mu\nu}, \quad \phi = -\lambda x, \quad f = 0, \quad (2.3)$$

satisfies the CGHS equations, cf. Appendix A.1. In this case the boundary $\phi = \phi_0$ is static, $x_{\text{boundary}} = -\phi_0/\lambda$, and the first of Eqs. (2.2) is automatically satisfied. Note that the Minkowski solution (2.3) appears in our model due to exact matching of the bulk and boundary terms with λ in the action (2.1).

2.2 Solution in the bulk and reflection laws

The CGHS equations in the bulk are exactly solvable [1, 2] in the light-cone frame (u, v) , where

$$ds^2 = -e^{2\rho(u,v)} du dv. \quad (2.4)$$

Let us review their general solution leaving technical details to Appendix A.2. In what follows we fix the remaining gauge freedom in Eq. (2.4) with the on-shell ‘‘Kruskal’’ condition $\rho = \phi$.

In the coordinates (2.4) the matter field satisfies $\partial_u \partial_v f = 0$ and therefore splits into a sum of incoming and outgoing parts,

$$f = f_{\text{in}}(v) + f_{\text{out}}(u) \quad (2.5)$$

The respective energy fluxes are

$$T_{vv}(v) = (\partial_v f_{\text{in}})^2 \quad \text{and} \quad T_{uu}(u) = (\partial_u f_{\text{out}})^2. \quad (2.6)$$

This specifies the Cauchy problem in our model: one prepares f_{in} or T_{vv} at the past null infinity and calculates f_{out} or T_{uu} at J^+ , see Fig. 1b.

The solution for the scale factor ρ and dilaton field ϕ is

$$e^{-2\rho} = e^{-2\phi} = -\lambda^2 vu + g(v) + h(u) , \quad (2.7)$$

where

$$g(v) = \frac{1}{2} \int_0^v dv' \int_{v'}^{+\infty} dv'' T_{vv}(v'') , \quad h(u) = -\frac{1}{2} \int_{-\infty}^u du' \int_{-\infty}^{u'} du'' T_{uu}(u'') . \quad (2.8)$$

We fixed the integration constants in these expressions by requiring, first, that the space-time is flat in the infinite past, i.e. no white hole preexists the scattering process. Second, we chose the coordinates in such a way that the quadrant $u \in (-\infty; 0)$, $v \in (0; +\infty)$ covers all space-time accessible to the distant observer. In particular, the limits $u \rightarrow -\infty$ at $v > 0$ and $v \rightarrow +\infty$ at $u < 0$ lead to J^- and J^+ , respectively, see Fig. 3.

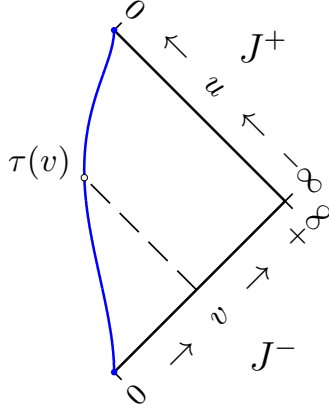


Figure 3. Penrose diagram showing the ranges of u , v and definition of $\tau(v)$.

Now, consider the boundary $\phi = \phi_0$ described by the function $u = U(v)$ in the “Kruskal” coordinates. Substituting the bulk solution (2.5), (2.7) into the boundary conditions (2.2), one obtains equation for $U(v)$ and reflection law for the matter field f ,

$$\frac{dU}{dv} = \frac{e^{2\phi_0}}{\lambda^2} (\partial_v g - \lambda^2 U)^2 , \quad f_{out}(U(v)) = f_{in}(v) , \quad (2.9)$$

see Appendix A.2 for the derivation of these equations and proof that they are compatible with the definition $\phi(U(v), v) = \phi_0$ of the boundary. Note that the second of Eqs. (2.9) relates the incoming and outgoing waves by conformal transformation $v \rightarrow U(v)$. The first equation implies that the boundary is always time-like,

$dU/dv > 0$. When rewritten in the appropriate terms, it coincides⁴ with the boundary equation obtained in [33, 34, 38] from energy conservation.

One easily finds solution in the empty space using Eqs. (2.9) and (2.7) with $T_{vv} = T_{uu} = 0$,

$$U(v) = -e^{-2\phi_0}/(\lambda^2 v), \quad e^{-2\rho} = e^{-2\phi} = -\lambda^2 uv, \quad f = 0, \quad (2.10)$$

where the integration constant in the first expression was chosen to make $U(v)$ smooth and invertible in the interval $0 < v < +\infty$. Solution (2.10) is the linear dilaton vacuum⁵: coordinate transformation

$$\lambda v = e^{\lambda(t+x)}, \quad \lambda u = -e^{-\lambda(t-x)} \quad (2.11)$$

brings it to the standard form (2.3). In what follows we impose flat asymptotics (2.10) in the infinite past $v \rightarrow 0$.

Note that the space-time (2.7) is always flat far away from the boundary, i.e. at large $|u|$ and v . Below we transform to the asymptotic Minkowski coordinates (t, x) using Eq. (2.11).

At this point, we have a receipt for solving the Cauchy problem in the CGHS model with a boundary. In this case the initial Cauchy data are represented by the incoming wave $f_{in}(v)$ or its energy flux $T_{vv}(v)$. One solves Eqs. (2.9) with the initial condition (2.10) at $v \rightarrow 0$ and finds $U(v)$, $f_{out}(u)$. The scale factor of the metric, dilaton and matter fields are then given by Eqs. (2.7) and (2.5).

2.3 Simple equation for the boundary

One notices that Eq. (2.9) for $U(v)$ is, in fact, a Riccati equation. The standard substitution

$$\lambda^2 U = \partial_v g - e^{-2\phi_0} \partial_v \psi / \psi, \quad (2.12)$$

brings it to the form of a Schrödinger equation for the new unknown $\psi(v)$,

$$\partial_v^2 \psi(v) = -\frac{e^{2\phi_0}}{2} T_{vv}(v) \psi(v). \quad (2.13)$$

Note that $\psi(v)$ is defined up to a multiplicative constant. Now, one can solve for $\psi(v)$ given the initial data $T_{vv}(v)$. After that the entire solution is determined by Eq. (2.12) and expressions from the previous Section. For example, the outgoing energy flux equals

$$T_{uu}(u) = \left(\lambda e^{\phi_0} \psi / \partial_v \psi \right)^4 T_{vv} \Big|_{v=V(u)}, \quad (2.14)$$

⁴It does not conform, however, with the “semiclassical” boundary conditions of [42–44] which, if imposed at the classical level, imply that the boundary is space-like.

⁵Recall that we excluded solutions with eternal black holes in Eq. (2.7).

where $V(u)$ is inverse of $U(v)$, $V(U(v)) = v$. We obtained Eq. (2.14) by substituting the reflection law (2.9) into the definition (2.6) of the flux and then expressing the derivative of $U(v)$ from the first of Eqs. (2.9) and Eq. (2.12).

Importantly, Eq. (2.13) is well-known in mathematical physics. Similar equation appears in Liouville theory at the classical and semiclassical levels [50]. Besides, the eigenstates of the Gaudin model [46] can be related to the solutions of Eq. (2.13) with monodromies ± 1 and rational T_{vv} [47]. In what follows we exploit these similarities for studying exact solutions in dilaton gravity.

The function $\psi(v)$ in Eq. (2.12) has simple geometric meaning. First, the value of ψ is related to the proper time τ along the boundary,

$$d\tau^2 = e^{2\phi_0} dU(v) dv = (\partial_v \psi / \lambda \psi)^2 dv^2 \quad \Rightarrow \quad \psi(v) = \psi_0 \cdot e^{\lambda \tau(v)}, \quad (2.15)$$

where we used Eqs. (2.4), (2.9), (2.12) in the second equality and introduced the arbitrary constant ψ_0 related to the origin of τ . Function $\tau(v)$ is illustrated in Fig. 3. Second, recall that v is the exponent of the flat light-cone coordinate $(t + u)$ far away from the boundary, Eq. (2.11). Thus, $\psi(v)$ maps the affine coordinate at J^- to τ . Equation (2.13) relates this coordinate-independent function to the asymptotic Cauchy data $T_{vv}(v)$.

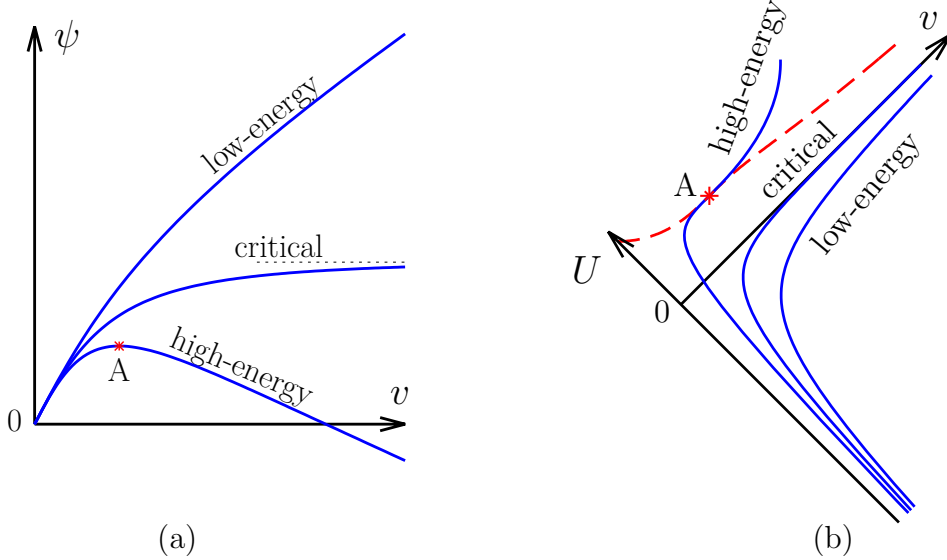


Figure 4. Functions $\psi(v)$ and $U(v)$ at different T_{vv} . The right graph is rotated for visualization purposes. Dashed line in this graph is the space-like “singularity” $\phi = \phi_0$.

Consider general properties of classical solutions in the model with a boundary. Relation (2.15) implies that $\psi(v)$ vanishes in the infinite past,

$$\psi(0) = 0. \quad (2.16)$$

Indeed, behavior $\psi \rightarrow c_0 v$ as $v \rightarrow 0$ corresponds to the linear dilaton vacuum (2.10) in the beginning of the process. To simplify the next argument, we set⁶ $c_0 = 1$. We consider well-localized $T_{vv}(v)$ and therefore linear asymptotics

$$\psi(v) \rightarrow Cv + D \quad \text{as} \quad v \rightarrow +\infty \quad (2.17)$$

of the solution to Eq. (2.13). If T_{vv} is small, one has $C \approx 1$. The respective “low-energy” solutions describe reflection of matter waves off the time-like boundary, see Figs. 4a,b. As T_{vv} grows, the function $\psi(v)$ becomes more concave and C decreases because $\partial_v^2 \psi \propto -T_{vv} < 0$. For some large fine-tuned $T_{vv}(v)$ one obtains critical solutions with $C = 0$. In this case the boundary is null in the asymptotic future because its proper time $\tau(v)$ in Eq. (2.15) remains finite as $v \rightarrow +\infty$. The respective “critical” solution in Figs. 4 is at the brink of black hole formation: we will see that the asymptotically null boundary sits precisely at the horizon of the smallest-mass black hole.

At sufficiently high energies we get $C < 0$ and therefore $\psi(v)$ has a maximum (point A in Fig. 4a). The boundary is null at this point: $dU/dv|_A \propto (\partial_v \psi)^2|_A = 0$ according to Eqs. (2.9) and (2.12). Moreover, near $A = (u_A, v_A)$ one obtains $U(v) \approx u_A + d \cdot (v - v_A)^3$ and

$$e^{-2\phi(u,v)} \approx e^{-2\phi_0} + \frac{T_{vv}(v_A)}{4d^{2/3}} [(u_A - u)^{2/3} - d^{2/3}(v - v_A)^2] .$$

where Eqs. (2.9), (2.12), and (2.7) were solved to the leading order in $u - u_A$, $v - v_A$. Thus, A is a singularity of $\phi(u, v)$.

Besides, one discovers that the condition $\phi = \phi_0$ defines *two* intersecting curves $u - u_A \approx \pm d(v - v_A)^3$ near A , and only one of those is the time-like boundary considered so far. The second curve is space-like, it is shown by the dashed line in Fig. 4b. We obtained the analog of the black hole singularity in the model with a boundary. Indeed, our model is formulated at $\phi < \phi_0$ i.e. in the space-time region to the right of both solid and dashed curves in Fig. 4b. The space-like “edge” $\phi = \phi_0$ swallows all matter at $u > 0$ limiting the region accessible to the outside observer to $u < 0$. The line $u = 0$ is a horizon.

Except for the point A itself, the solution is smooth at the space-like “singularity” $\phi = \phi_0$. This fact was not appreciated in the previous studies. The mass of the formed black hole, by energy conservation, is related to the value of the dilaton field at the future horizon,

$$M_{bh} = \int_0^{+\infty} \lambda v dv T_{vv} - \int_{-\infty}^0 \lambda |u| du T_{uu} = 2\lambda [g(+\infty) + h(0)] = 2\lambda \lim_{v \rightarrow +\infty} e^{-2\phi(0,v)} ,$$

⁶Recall that $\psi(v)$ is defined up to a multiplicative constant.

where we subtracted the final matter energy from the initial one in the first equality (cf. Eq. (2.11)), integrated by parts and used Eqs. (2.8) in the second equality, and then expressed the result in terms of ϕ , Eq. (2.7). Since $\phi < \phi_0$, this implies that all black hole masses are larger than

$$M_{cr} = 2\lambda e^{-2\phi_0} , \quad (2.18)$$

see detailed discussion in [5, 41]. Black holes with $M_{bh} = M_{cr}$ and boundary sitting precisely at the horizon are formed in the critical solutions.

The solutions in Fig. 4b, when replotted in the finite-range coordinates $(\bar{u}, \bar{v}) = (\arctan u, \arctan v)$, look like Penrose diagrams, see Fig. 2. From now on, we will use \bar{u} and \bar{v} for visualizing the solutions. We will also mark the (smooth) space-like “singularity” lines $\phi = \phi_0$ by zigzag lines, see the one in Fig. 2c.

2.4 On-shell conformal symmetry

Quite unexpectedly, we find that Eq. (2.13) is invariant under conformal transformations $v \rightarrow w(v)$,

$$\psi \rightarrow \tilde{\psi}(w) = \left(\frac{dv}{dw} \right)^{-1/2} \psi(v) , \quad (2.19)$$

$$T_{vv} \mapsto \tilde{T}_{vv}(w) = \left(\frac{dv}{dw} \right)^2 T_{vv}(v) + e^{-2\phi_0} \{v; w\} , \quad (2.20)$$

which change $\psi(v)$ as an $h = -1/2$ primary field and $T_{vv}(v)$ as an energy-momentum tensor with large negative central charge $c = -24\pi e^{-2\phi_0}$ [51]. In Eq. (2.19) we introduced the Schwarzian derivative $\{v; w\} \equiv v'''/v' - 3(v'')^2/2(v')^2$ with $v' \equiv dv/dw$.

The transformations (2.19), (2.20) relate physically distinct solutions⁷ with different energy fluxes T_{vv} . Although it may appear otherwise, Eq. (2.20) does not represent the asymptotic conformal transformations $f_{in} \rightarrow f_{in}(v(w))$ of the massless field f far away from the boundary. Indeed, unlike in Eq. (2.20) the classical asymptotic symmetry changes $T_{vv} \equiv (\partial_v f_{in})^2$ without the Schwarzian derivative. At the quantum level, healthy conformal matter has positive central charge $c > 0$ [51], and transformations of its energy-momentum tensor T_{vv} do not match Eq. (2.20) as well. The exceptions are $\text{SL}(2, \mathbb{R})$ transformations

$$v \rightarrow w(v) = \frac{\alpha v + \beta}{\gamma v + \delta} , \quad \alpha\delta - \beta\gamma = 1 , \quad (2.21)$$

which coincide in Eq. (2.20) and at the asymptotics due to the property $\{v; w\} = 0$. These transformations constitute the global $\text{SL}(2, \mathbb{R})$ symmetry group which is linearly realized from the viewpoints of both asymptotic and boundary observers.

⁷Unlike the transformations in [38, 39], they do not represent residual gauge symmetry.

As a side remark, let us argue that (2.19), (2.20) is the symmetry of the gravitational degrees of freedom “sitting” at the boundary. To this end we introduce the field $\chi(u) = e^{-\lambda\tau(u)}/\psi_0$ which is T -symmetric with respect to $\psi(v)$ and therefore satisfies

$$\partial_u^2 \chi(u) = -\frac{e^{2\phi_0}}{2} T_{uu}(u) \chi(u) , \quad (2.22)$$

cf. Eqs. (2.15) and (2.13); now, $\tau(u)$ is the boundary proper time parametrized with u . It is convenient to combine $\psi(v)$ and $\chi(u)$ into a single free field

$$e^{-2\Phi(u,v)} \equiv \chi(u) \psi(v) e^{-2\phi_0} ,$$

transforming in a simple Liouville-like manner under Eq. (2.19). Since we introduced Φ to describe the gravitational degrees of freedom, it is natural to extract its energy-momentum tensor from Einstein equations $T_{\mu\nu}^{(\Phi)} + T_{\mu\nu} = 0$,

$$T_{vv}^{(\Phi)} \equiv -T_{vv} = 8e^{-2\phi_0} [(\partial_v \Phi)^2 - \partial_v^2 \Phi/2] , \quad T_{uu}^{(\Phi)} \equiv -T_{uu} ,$$

where Eq. (2.13) was used in the left equality; similar expression for $T_{uu}^{(\Phi)}$ can be obtained using Eq. (2.22). One observes that $T_{vv}^{(\Phi)}$ transforms under Eq. (2.19) as an energy-momentum tensor with positive conformal charge $c = 24\pi e^{2\phi_0}$, in exact agreement with Eq. (2.20).

Now, the entire scattering problem can be reformulated in terms of the boundary field Φ . One sends the incoming energy flux $T_{vv}^{(\Phi)}$ towards the dynamical boundary $u = U(v)$ at $\Phi = \phi_0$. The flux reflects into $T_{uu}^{(\Phi)}$ according to the non-conformal law $T_{uu}^{(\Phi)} = (dU/dv)^{-2} T_{vv}^{(\Phi)}$, Eq. (2.14). In this setup⁸ Eqs. (2.19), (2.20) constitute the apparent conformal symmetry of Φ far away from the boundary, whereas the symmetry of the matter sector is hidden in the reflection laws.

3 Integrable sector

3.1 General solution

One can use Eq. (2.13) to express the entire solution in terms of one arbitrary function. Indeed, introducing

$$W \equiv \partial_v \psi / \psi = e^{2\phi_0} (\partial_v g - \lambda^2 U) , \quad (3.1)$$

we find,

$$\psi = e^{\int^{v} dv' W(v')} , \quad -\frac{e^{2\phi_0}}{2} T_{vv} = W^2 + \partial_v W . \quad (3.2)$$

Then U , T_{uu} , ϕ , and f are given by Eqs. (3.1), (2.14), (2.7), and (2.6). We obtained general solution in the model with a boundary.

⁸Note that all equations and boundary conditions for Φ can be summarized in the flat-space action $S_\Phi = -\int_{\Phi < \phi_0} d^2x [e^{-2\phi_0} (\partial_\mu \Phi)^2 + \lambda^2]$.

By itself, this solution is of little practical use because the function $\psi(v)$ has a zero at $v = 0$ and, possibly, another one at $v = \tilde{v}_1 > 0$, see Fig. 4a. In general, the incoming flux $T_{vv}(v)$ in Eq. (3.2) is singular at these points. Indeed, Eq. (3.1) gives

$$W(v) = R(v) + 1/v + 1/(v - \tilde{v}_1) ,$$

where $R(v)$ is regular at $v \geq 0$, and therefore $T_{vv}(v)$ has first-order poles at $v = 0$ and \tilde{v}_1 . Requiring zero residuals at these poles, we obtain two constraints $R(0) = -R(\tilde{v}_1) = 1/\tilde{v}_1$ on parameters of $R(v)$.

Choosing multiparametric $R(v)$ and solving the constraints, one finds an arbitrary number of smooth solutions. The physical ones satisfy

$$T_{vv}(v) \geq 0 , \quad \text{at} \quad v \geq 0 . \quad (3.3)$$

In what follows we will concentrate on a large class of soliton solutions with power-law singularities. We will argue that some of them satisfy Eq. (3.3).

3.2 Soliton solutions with power-law singularities

Let us follow the Painlevé test [52] and guess the form of $T_{vv}(v)$ which guarantees that the general solution $\psi(v)$ of Eq. (2.13) has power-law singularities $\psi \sim (v - v_0)^{-s}$ in the complex v -plane. One introduces the Laurent series at $v \approx v_0$,

$$-\frac{e^{2\phi_0}}{2} T_{vv} = \sum_{k=0}^{+\infty} T_{k-2}(v - v_0)^{k-2} , \quad \psi = \sum_{k=0}^{+\infty} \psi_{k-s}(v - v_0)^{k-s} , \quad (3.4)$$

where the expansion of T_{vv} starts from $(v - v_0)^{-2}$ due to Eq. (2.13). Substituting Eqs. (3.4) into Eq. (2.13), we obtain an infinite algebraic system for ψ_{k-s} ,

$$(k - s)(k - s - 1)\psi_{k-s} = T_{-2}\psi_{k-s} + T_{-1}\psi_{k-s-1} + \cdots + T_{k-2}\psi_{-s} . \quad (3.5)$$

The very first ($k = 0$) of these relations gives $T_{-2} = s(s + 1)$, the others determine ψ_{k-s} with $k \geq 1$ in terms of arbitrary ψ_{-s} and $\{T_m\}$. Expression (3.4) represents general solution of the second-order equation (2.13) if precisely two of its parameters, ψ_{-s} and some ψ_{k_0-s} , remain arbitrary. Thus, $(k_0 - s)(k_0 - s - 1) = s(s + 1)$ in Eq. (3.5), leading to $k_0 = 2s + 1$. One concludes that s is integer or half-integer.

Note that the two equations from the system (3.5) which do not determine the coefficients of ψ , constrain $\{T_k\}$. For example for $s = 1/2$ one gets,

$$T_{-2} = 3/4 , \quad T_0 = (T_{-1})^2 , \quad (3.6)$$

where we expressed all $\psi_{k-1/2}$ via T_k and $\psi_{-1/2}$. For larger s , one obtains $T_{-2} = s(s + 1)$ and higher-order equations listed in Table 1.

We arrived at the practical method for obtaining the soliton solutions in our model. One specifies N singularities of $\psi(v)$: selects their integer or half-integer

s	equation
1	$T_1 = T_0 T_{-1} - \frac{1}{4}(T_{-1})^3$
3/2	$T_2 = \frac{2}{3}T_1 T_{-1} - \frac{5}{18}T_0(T_{-1})^2 + \frac{1}{4}(T_0)^2 + \frac{1}{36}(T_{-1})^4$
2	\dots

Table 1. Equations for the Laurent coefficients of the solitonic $T_{vv}(v)$.

powers s_n and complex positions v_n . The function $T_{vv}(v)$ has second-order poles at $v = v_n$, see Eq. (3.4). This analytic structure gives expressions,

$$-\frac{e^{2\phi_0}}{2}T_{vv} = \sum_{n=1}^N \left[\frac{s_n(s_n+1)}{(v-v_n)^2} + \frac{T_{-1}^n}{v-v_n} \right], \quad \psi = C \frac{\prod_{m=1}^M (v - \tilde{v}_m)}{\prod_{n=1}^N (v - v_n)^{s_n}}, \quad (3.7)$$

where we required $T_{vv} \rightarrow 0$ as $v \rightarrow +\infty$ and introduced a polynomial in the nominator of $\psi(v)$ with M zeroes \tilde{v}_m and a normalization constant C . Next, one solves equations in Table 1 at each singularity and determines T_{-1}^n . After that $\psi(v)$ is obtained by substituting Eqs. (3.7) into Eqs. (2.13) or (3.5). Two parameters — say, C and \tilde{v}_M — remain arbitrary because Eq. (3.7) is a general solution of the second-order equation. One takes $\tilde{v}_M = 0$ in accordance with the flat-space asymptotics (2.16). This gives the solutions $\{\psi(v), T_{vv}(v)\}$ characterized by N complex parameters v_n and the same number of integers or half-integers s_n .

We consider solutions with finite total energy of incoming matter,

$$E_{in} = \int_0^{+\infty} \lambda v dv T_{vv}(v),$$

see Eq. (2.11). Convergence of this integral implies $T_{vv} \sim \bar{o}(v^{-2})$ as $v \rightarrow +\infty$ or, given Eq. (3.7), linear relations

$$\sum_{n=1}^N T_{-1}^n = 0, \quad \sum_{n=1}^N [s_n(s_n+1) + v_n T_{-1}^n] = 0. \quad (3.8)$$

Moreover, the asymptotic (2.17) of $\psi(v)$ suggests falloff $T_{vv} \sim O(v^{-4})$ at large v and additional relation

$$\sum_{n=1}^N [2v_n s_n(s_n+1) + v_n^2 T_{-1}^n] = 0, \quad (3.9)$$

which should hold for noncritical solutions. Equations (3.8), (3.9) are useful for obtaining the lowest solitons.

Example. Consider the solution with two $s = 1/2$ singularities⁹. Solving the finite-energy conditions (3.8), one obtains $T_{-1}^1 = -T_{-1}^2 = 3/[2(v_2 - v_1)]$. It is straightforward to check that $T_{vv}(v)$ with these parameters satisfies Eqs. (3.6) at $v = v_1$ and

⁹Note that $T_{vv}(v)$ with one singularity does not satisfy the conditions (3.8).

$v = v_2$. To make the solution real at $v \in \mathbb{R}$, we take $v_1 = a + ib$ and $v_2 = a - ib$. Then Eqs. (3.7) take the form,

$$T_{vv} = \frac{6e^{-2\phi_0} b^2}{[(v-a)^2 + b^2]^2}, \quad \psi(v) = \frac{v(a^2 + b^2 - av)}{[(v-a)^2 + b^2]^{1/2}}, \quad (3.10)$$

where $\psi(v)$ was obtained by substituting Eqs. (3.7) into Eq. (2.13). One observes that the matter flux (3.10) peaks near $v \sim a$, its total energy $E_{in} = \frac{3}{2}M_{cr} [1 + \frac{a}{b} \operatorname{arctg}(-a/b)]$ is controlled by the ratio a/b , where $M_{cr} = 2\lambda e^{-2\phi_0}$ is the minimal black hole mass.

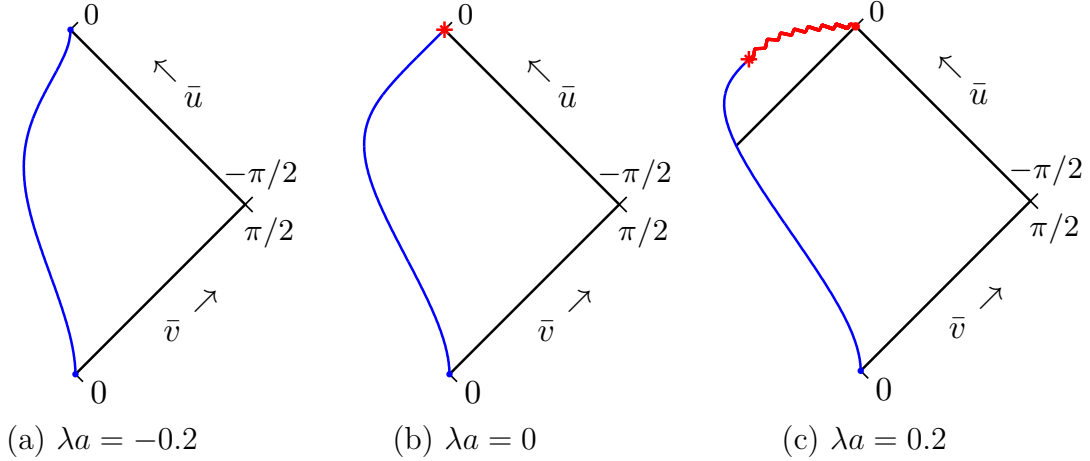


Figure 5. Solution (3.10) in the finite-range coordinates $\bar{u} = \operatorname{arctg}(\lambda u)$, $\bar{v} = \operatorname{arctg}(\lambda v)$ at different values of a . We use $\lambda b = e^{2\phi_0} = 1$ keeping in mind that the parameter $e^{2\phi_0} \ll 1$ can be restored in the classical solution, see discussion in Sec. 2.1.

Since $\psi \rightarrow -av$ as $v \rightarrow +\infty$, the solutions (3.10) describe reflection of matter waves off the boundary and formation of black holes at $a < 0$ and $a > 0$, respectively, see Fig. 4a. This fact is clearly seen in Fig. 5 showing the boundary $u = U(v)$ at different a in the finite-range coordinates (\bar{u}, \bar{v}) . In Fig. 5c we also plotted the space-like “singularity” $\phi = \phi_0$ and horizon $u = 0$ (zigzag red and solid black lines, respectively).

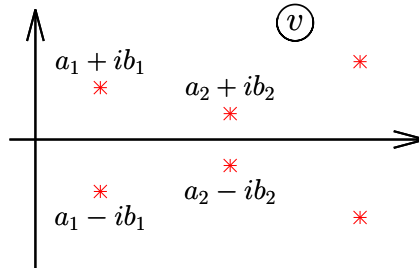


Figure 6. Singularities of the exact solutions in the complex v -plane.

The simplest exact solution in Eq. (3.10) describes the incoming matter flux with a single peak. Solutions with multiple peaks can be obtained by adding singularities at $v = a_n \pm ib_n$, see Fig. 6. Unfortunately, it is hard to find these solutions explicitly at large N . Besides, it is not clear whether they will satisfy the positivity condition (3.3). We will clarify these issues in the subsequent Sections.

3.3 Simplifying the coefficient equations

Instead of solving the equations in Table 1, one can extract $T_{vv}(v)$ from the general solution. Namely, substituting the solitonic $\psi(v)$ into the first of Eqs. (3.2), we find,

$$W(v) = - \sum_{n=1}^N \frac{s_n}{v - v_n} + \sum_{m=1}^M \frac{1}{v - \tilde{v}_m} . \quad (3.11)$$

Then the second of Eqs. (3.2) gives the incoming flux. However, in this case $T_{vv}(v)$ receives parasitic first-order poles at $v = \tilde{v}_m$ which are absent in Eq. (3.7). Requiring zero residuals at these poles, we obtain equations for $\{\tilde{v}_m\}$,

$$\sum_{n=1}^N \frac{s_n}{\tilde{v}_m - v_n} = \sum_{\substack{m'=1 \\ m' \neq m}}^M \frac{1}{\tilde{v}_m - \tilde{v}_{m'}} , \quad (3.12)$$

which are, in fact, equivalent to the ones in Table 1. Indeed, after solving Eqs. (3.12) one obtains $T_{vv}(v)$ of the form (3.7) with

$$T_{-1}^n = \sum_{n' \neq n} \frac{2s_n s_{n'}}{v_n - v_{n'}} - \sum_m \frac{2s_n}{v_n - \tilde{v}_m} . \quad (3.13)$$

In practice, one finds \tilde{v}_m numerically from Eqs. (3.12), then computes T_{vv} and ψ by Eqs. (3.13) and (3.7).

Unlike in Sec. 3.1, we impose Eqs. (3.12) at all \tilde{v}_m , not just the ones at the real positive axis. The goal is to obtain solutions with transparent properties which will be considered in Sec. 3.5.

3.4 $\text{SL}(2, \mathbb{C})$ symmetry

The global $\text{SL}(2, \mathbb{C})$ transformations (2.21) are invertible and therefore preserve the singularity structure of the solitons. One obtains,

$$T_{vv} \rightarrow \tilde{T}_{vv}(w) = \frac{T_{vv}(v)}{(\alpha - \gamma w)^4} , \quad \psi \rightarrow \tilde{\psi}(w) = (\alpha - \gamma w) \psi(v) . \quad (3.14)$$

These transformations relate solitons with different parameters. Real solutions at $v \geq 0$ have $\text{SL}(2, \mathbb{R})$ symmetry.

The transformation (2.21) sends the point $v = -\delta/\gamma$ to infinity. If the original solution is regular at this point, its image receives asymptotics $\tilde{\psi} \rightarrow Cw + D$ and

$\tilde{T}_{vv} \rightarrow O(w^{-4})$ as $w \rightarrow +\infty$. In Eq. (2.17) we obtained the same asymptotics from physical considerations. Solutions with other asymptotics, i.e. those violating the finite-energy conditions (3.8) or Eq. (3.9), have singularities “sitting” at infinity.

Example. One can use the above property to construct new solutions. Consider e.g. the trivial solution $\psi = v^{-s} - v^{s+1}$, $T_{vv} = -2e^{-2\phi_0} s(s+1)/v^2$ of Eq. (2.13) with non-linear $\psi(v)$ at large v . We send the points $v = 0, \infty$, and 1 to v_1, v_2 , and 0 by linear rational transformation¹⁰ (3.14) and get,

$$T_{vv} = \frac{-2e^{-2\phi_0} s(s+1)(v_2 - v_1)^2}{(v - v_1)^2(v - v_2)^2}, \quad \psi = \frac{i(v - v_1)^{s+1}v_2^s}{v_1^{s+1}(v - v_2)^s} - \frac{i(v - v_2)^{s+1}v_1^s}{v_2^{s+1}(v - v_1)^s}, \quad (3.15)$$

where the constant in front of $\psi(v)$ was ignored. This is the soliton with two singularities. Taking $v_1 = v_2^* = a + ib$, one obtains $T_{vv}(v) \geq 0$ at real v . Note that the incoming flux in Eq. (3.15) is the same as in Eq. (3.10) albeit with different multiplicative factor. The behaviors of the boundaries are also similar, as one can see by comparing the solutions (3.15) with¹¹ $s = 1/2$ and 1 in Figs. 5 and 2, respectively.

3.5 Relation to the Gaudin model

In this Section we establish one-to-one correspondence between the solitons (3.7) and eigenstates of the auxiliary integrable system, the Gaudin model [46–48]. This will allow us to count the number of solitons and explain some of their properties.

The Gaudin model [46] describes a chain of N three-dimensional spins $\hat{\mathbf{s}}_n = \{s_n^1, s_n^2, s_n^3\}$ with the standard commutation relations $[\hat{s}_n^\alpha, \hat{s}_l^\beta] = i\delta_{nl} \epsilon^{\alpha\beta\gamma} \hat{s}_n^\gamma$. The model is equipped with N commuting Hamiltonians

$$\hat{\mathcal{T}}_n = \sum_{l \neq n} \frac{(\hat{\mathbf{s}}_n, \hat{\mathbf{s}}_l)}{v_n - v_l}, \quad (3.16)$$

where v_n are complex parameters and $(\hat{\mathbf{s}}_n, \hat{\mathbf{s}}_l) \equiv \sum_\alpha \hat{s}_n^\alpha \hat{s}_l^\alpha$ is the scalar product. The eigenstates $|\Psi\rangle$ of the model simultaneously diagonalize all Hamiltonians, $\hat{\mathcal{T}}_n|\Psi\rangle = \mathcal{T}_n|\Psi\rangle$, where \mathcal{T}_n are complex eigenvalues.

It is convenient to pack all spins and Hamiltonians into the operator-valued functions

$$\hat{\mathbf{s}}(v) \equiv \sum_{n=1}^N \frac{\hat{\mathbf{s}}_n}{v - v_n}, \quad \hat{\mathcal{T}}(v) \equiv [\hat{\mathbf{s}}(v)]^2 = \sum_{n=1}^N \left[\frac{\hat{\mathbf{s}}_n^2}{(v - v_n)^2} + \frac{2\hat{\mathcal{T}}_n}{v - v_n} \right]. \quad (3.17)$$

Now, the eigenvectors satisfy $\hat{\mathcal{T}}(v)|\Psi\rangle = \mathcal{T}(v)|\Psi\rangle$.

A complete set of eigenvectors and eigenvalues in the model (3.16) is provided by the algebraic Bethe Ansatz [46–48]. We review this method in Appendix B and list its main results below.

¹⁰With parameters $\alpha = -\beta = (1/v_2 - 1/v_1)^{-1/2}$, $\gamma = \alpha/v_2$, $\delta = \beta/v_1$.

¹¹In Figs. 2a, b, and c we used $\lambda a = -1, -1/\sqrt{3}$, and 0.3 , respectively, and $\lambda b = e^{-2\phi_0} = 1$.

One fixes the representations $(\hat{\mathbf{s}}_n)^2 = s_n(s_n + 1)$ of all spins, where s_n are integers or half-integers. The simplest eigenstate $|0\rangle$ of the Gaudin model has all spins down,

$$\hat{s}_n^-|0\rangle = 0, \quad \hat{s}_n^3|0\rangle = -s_n|0\rangle \quad \text{for all } n, \quad (3.18)$$

where $s_n^- \equiv s_n^1 - i s_n^2$ are the lowering operators. The other eigenstates are obtained by acting on $|0\rangle$ with rising operators $\hat{s}^+(v) \equiv \hat{s}^1(v) + i \hat{s}^2(v)$,

$$|\tilde{v}_1, \dots, \tilde{v}_M\rangle = \hat{s}^+(\tilde{v}_1)\hat{s}^+(\tilde{v}_2)\dots\hat{s}^+(\tilde{v}_M)|0\rangle \quad (3.19)$$

at certain points \tilde{v}_m which satisfy the Bethe equations,

$$-\sum_{n=1}^N \frac{s_n}{\tilde{v}_m - v_n} + \sum_{\substack{m'=1 \\ m' \neq m}}^M \frac{1}{\tilde{v}_m - \tilde{v}_{m'}} = 0. \quad (3.20)$$

The eigenvalue of $\hat{\mathcal{T}}(v)$ corresponding to the state (3.19) is

$$\mathcal{T}(v) = W^2 + \partial_v W, \quad W(v) = -\sum_{n=1}^N \frac{s_n}{v - v_n} + \sum_{m=1}^M \frac{1}{v - \tilde{v}_m}. \quad (3.21)$$

To sum up, one solves Eqs. (3.20) for every M and finds all $\prod_n (2s_n + 1)$ eigenvectors and eigenvalues of $\hat{\mathcal{T}}(v)$.

Importantly, the Bethe equations (3.20) coincide with the algebraic equations (3.12) for the parameters \tilde{v}_m of the solitons in dilaton gravity. This establishes one-to-one correspondence between our exact solutions and the eigenstates (3.19) of the Gaudin model. The singularities $\{s_n, v_n\}$ and zeros $\{\tilde{v}_m\}$ of $\psi(v)$ are related to the parameters of the Gaudin Hamiltonians (3.16) and Bethe states (3.19), respectively. Besides, the incoming flux $T_{vv}(v)$ is proportional to the eigenvalue of $\hat{\mathcal{T}}(v)$: $T_{vv}(v) = -2e^{-2\phi_0} \mathcal{T}(v)$, cf. Eqs. (3.2), (3.11) and (3.21). The related quantities of the two models are listed in Table 2.

	Solitons	Eigenstates of the Gaudin model
v_n	positions of singularities	parameters of the Hamiltonians
s_n	powers of singularities	representations of $\hat{\mathbf{s}}_n$
\tilde{v}_m	zeros of $\psi(v)$	parameters of eigenstates
$T_{vv} = -\frac{e^{-2\phi_0}}{2} \mathcal{T}$	incoming energy flux	eigenvalue of $\hat{\mathcal{T}}(v)$
$T_{-1}^n = 2\mathcal{T}_n$	coefficients of T_{vv}	eigenvalues of $\hat{\mathcal{T}}_n$

Table 2. Correspondence between the solitons in dilaton gravity and eigenstates of the Gaudin model.

One can use the Gaudin model to study solutions in dilaton gravity. We are interested in well-localized solitons with $T_{vv} = O(v^{-4})$ as $v \rightarrow +\infty$. The corresponding

Gaudin states have zero total spin¹²

$$\hat{\mathbf{S}} = \sum_n \hat{\mathbf{s}}_n$$

because $\hat{\mathcal{T}} \rightarrow (\hat{\mathbf{S}}/v)^2$ as $v \rightarrow +\infty$, see Eq. (3.17). Using this property, one counts the number of the solitons with correct asymptotics by adding up spins. For example, there are two such solutions with four $s = 1/2$ singularities because the Hilbert space of four $s = 1/2$ spins has two-dimensional zero- $\hat{\mathbf{S}}$ subspace: $(1/2)^{\otimes 4} = 0 \oplus 0 \oplus 1 \oplus 1 \oplus 1 \oplus 2$, where the spin representations are marked with their highest weights.

Besides, now we can explain what happens at $v_1 \rightarrow v_2$ when two singularities of the solutions coalesce. In this limit the spin operator (3.17),

$$\hat{\mathbf{s}}(v) \rightarrow \frac{\hat{\mathbf{s}}_1 + \hat{\mathbf{s}}_2}{v - v_2} + \sum_{n \geq 3} \frac{\hat{\mathbf{s}}_n}{v - v_n} \quad \text{as } v_1 \rightarrow v_2 ,$$

depends on the sum $\hat{\mathbf{s}}_1 + \hat{\mathbf{s}}_2$. The corresponding solutions have singularities at $v = v_2$ of powers $|s_1 - s_2|$, $|s_1 - s_2| + 1$, \dots , $(s_1 + s_2)$ in accordance with the irreducible representations of $\hat{\mathbf{s}}_1 + \hat{\mathbf{s}}_2$. For instance, consider coalescence of two $s_{1,2} = 1/2$ singularities as $v_1 \rightarrow v_2$. The second-order equations (3.6) at these singularities have four solutions representing four eigenstates of two $s = 1/2$ spins. In the limit $v_1 \rightarrow v_2$ the spins sum up and we obtain¹³ one $s = 0$ (non-singular) solution and three solutions with $s = 1$ singularity.

Finally, one can obtain more general solutions with infinite number of singularities using the thermodynamic Bethe Ansatz for the Gaudin model [53].

Example. Consider the solution with four $s = 1/2$ singularities arranged in the two complex conjugate pairs $v_{1,2} = a_1 \pm ib_1$, $v_{3,4} = a_2 \pm ib_2$. Solving Eqs. (3.8), (3.9), (3.6), we obtain, as expected above, two solutions

$$T_{vv}^{(\pm)} = \frac{6b_1^2 e^{-2\phi_0}}{((v - a_1)^2 + b_1^2)^2} + \frac{6b_2^2 e^{-2\phi_0}}{((v - a_2)^2 + b_2^2)^2} - 2e^{-2\phi_0} \frac{(a_1 - a_2)^2 + b_1^2 + b_2^2 \pm \sqrt{\Delta}}{((v - a_1)^2 + b_1^2)((v - a_2)^2 + b_2^2)} , \quad (3.22)$$

where $\Delta = ((a_1 - a_2)^2 + b_1^2 + b_2^2)^2 + 12b_1^2 b_2^2 > 0$. In the limit $a_1 \rightarrow a_2$, $b_1 \rightarrow b_2$ the pairs of singularities in the upper and lower parts of the complex v -plane coalesce, and one obtains a nonsingular solution and a solution (3.15) with two $s = 1$ singularities,

$$T_{vv}^{(+)} \rightarrow 0 , \quad T_{vv}^{(-)} \rightarrow \frac{16e^{-2\phi_0} b_2^2}{((v - a_2)^2 + b_2^2)^2} ,$$

again in accordance with the above expectations.

¹²Note that $\hat{\mathbf{S}}$ commutes with all Gaudin Hamiltonians.

¹³One can explicitly demonstrate this by solving Eqs. (3.6) to the leading order in $v_1 - v_2 \rightarrow 0$.

Note that $T_{vv}^{(+)}(v)$ is not positive-definite at real positive v and therefore unphysical. The function $T_{vv}^{(-)}(v)$ describes incoming matter flux with two peaks at $v \sim a_1$ and a_2 , see Fig. 7.

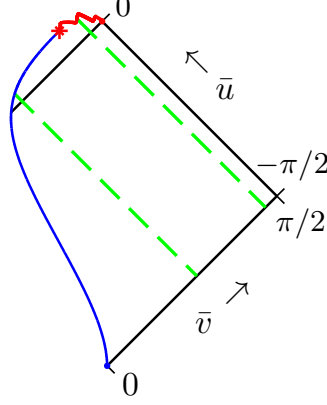


Figure 7. Solution “-” in Eq. (3.22) with four $s = 1/2$ poles and parameters $\lambda a_1 = -0.1$, $\lambda b_1 = 1$, $\lambda a_2 = 0.2$, $\lambda b_2 = 10$, and $e^{-2\phi_0} = 1$. The two peaks of the incoming matter flux are marked by the dashed lines.

3.6 Positivity condition

Physical solutions have real $\psi(v)$ at real v . Thus, their singularities v_n and zeros \tilde{v}_m are either real or organized in complex conjugate pairs like in Fig. 6. Besides, the singularities v_n may not be placed at the physical part $v \geq 0$ of the real axis.

The only nontrivial condition is $T_{vv}(v) \geq 0$ at $v \geq 0$, Eq. (3.3). This inequality is not satisfied automatically. For example, our solutions with two singularities (3.15) have negative and positive $T_{vv}(v)$ at $v_{1,2} < 0$ and $v_{1,2} = a \pm ib$, respectively. In fact, any solution with all singularities placed at $v < 0$ is unphysical. In this case the operator $\hat{\mathbf{s}}(v)$ at real v is Hermitean, and therefore $\hat{\mathcal{T}}(v)$ in Eq. (3.17) has positive-definite eigenvalues $\mathcal{T}(v) \propto -T_{vv}(v)$.

In the opposite case when all singularities are organized in complex conjugate pairs $v_{2k-1}, v_{2k} = a_k \pm ib_k$, one expects to find at least one physical solution. Indeed, consider the state $|\Psi_1\rangle$ (not an eigenstate) of the Gaudin model satisfying $(\hat{\mathbf{s}}_{2k-1} + \hat{\mathbf{s}}_{2k})|\Psi_1\rangle = 0$ for all k . Explicit calculation shows that $\langle \Psi_1 | \hat{\mathcal{T}}(v) | \Psi_1 \rangle < 0$ at real v . On the other hand, the variational principle implies that for any N real points w_n there exists an eigenstate $|\Psi\rangle$ minimizing all $\langle \Psi | \hat{\mathcal{T}}(w_n) | \Psi \rangle$. The respective eigenvalue $\mathcal{T}(v)$ is negative at all $v = w_n$ suggesting that $T_{vv}(v) \propto -\mathcal{T}(v)$ is positive at the entire real axis.

Let us explicitly select the above physical solution at $b_k \rightarrow 0$. In this case $T_{vv}(v)$ falls into a collection of peaks at $v \sim a_k$ near the singularities v_{2k-1}, v_{2k} . At $|v - a_k| \gg b_k$ and yet, far away from other singularities, the operator (3.17) takes the form $\hat{\mathcal{T}}(v) \approx (\hat{\mathbf{s}}_{2k-1} + \hat{\mathbf{s}}_{2k})^2 / (v - a_k)^2$. Its eigenvalue $\mathcal{T}(v) \propto -T_{vv}(v)$ is

positive-definite unless the eigenstate satisfies $(\hat{s}_{2k-1} + \hat{s}_{2k})|\Psi\rangle = 0$. Thus, in the limit $b_k \rightarrow 0$ the physical eigenstate coincides with the state $|\Psi_1\rangle$ introduced above. The respective energy flux $T_{vv}(v)$ is the sum of the two-spin terms (3.15),

$$T_{vv} \approx 8e^{-2\phi_0} \sum_{k=1}^{N/2} \frac{s_{2k}(s_{2k} + 1)b_k^2}{[(v - a_k)^2 + b_k^2]^2} \quad \text{at small } b_k.$$

One expects that this solution remains physical at finite b_k .

Example. In general case, the positivity condition bounds the parameters of the solutions. Consider e.g. the soliton with three $s = 1$ singularities at $v_{1,2} = a \pm ib$, $v_3 < 0$, see Fig. 8a. Solving Eqs. (3.8), (3.9), one obtains,

$$T_{vv} = \frac{16e^{-2\phi_0}b^2}{((v - a)^2 + b^2)^2} - \frac{4e^{-2\phi_0}[(a - v_3)^2 + b^2]}{(v - v_3)^2[(v - a)^2 + b^2]}. \quad (3.23)$$

The second (negative) term in this expression represents contribution of the singularity $v_3 < 0$. It can be compensated by the first term if the singularities v_1 and v_2 are close enough to v_3 . Namely, the function (3.23) is positive-definite at $v \geq 0$ if $a - b\sqrt{3} \leq v_3 \leq (a^2 + b^2)/(a - b\sqrt{3})$, see the gray region in Fig. 8b. Unfortunately, the solutions with these parameters involve one peak of the incoming flux, just like the solutions (3.15).

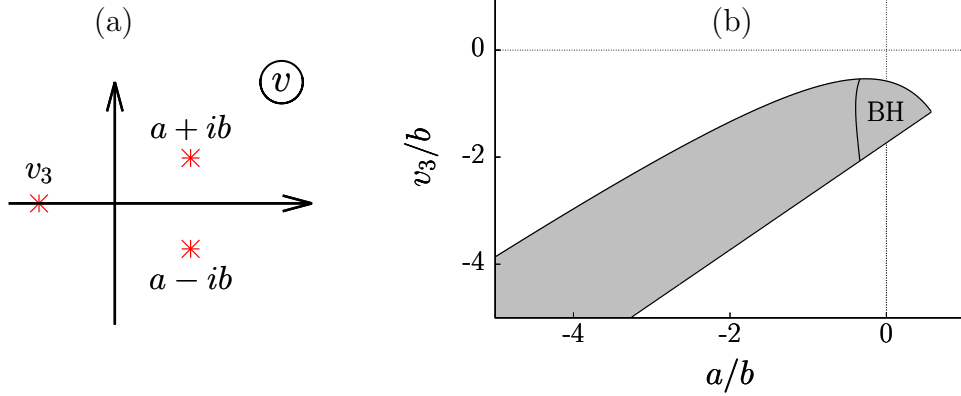


Figure 8. (a) Singularities of the solution (3.23). (b) Parameters of this solution giving positive-definite $T_{vv}(v)$ at $v \geq 0$ (gray region). The upper right corner of the allowed region corresponds to black hole formation.

4 Critical chaos

4.1 Perturbative expansion in the critical regime

In Sec. 2.3 we argued that the critical solutions corresponding to the verge of black hole formation have constant $\psi(v)$ and null boundary $U(v)$ at large v , see Fig. 4.

One can say that they describe formation of the minimal-mass black holes with the boundary placed precisely at the horizon [54][45], cf. [55, 56].

At energies somewhat below critical the boundary has long almost null part (“plateau”), see Fig. 9a. The energy flux reflected from this part is strongly amplified by the Lorentz factor of the boundary and forms a high and narrow peak in $T_{uu}(u)$, see Fig. 9b. We will argue below that in the critical limit the peak tends to a δ -function (“thunderpop”) with energy equal to the minimal black hole mass M_{cr} . In the overcritical solutions the “thunderpop” is swallowed by the black hole. Besides, we will see in the next Section that the structure of the peak is highly sensitive to the initial data. This feature may impede global integrability of the model.

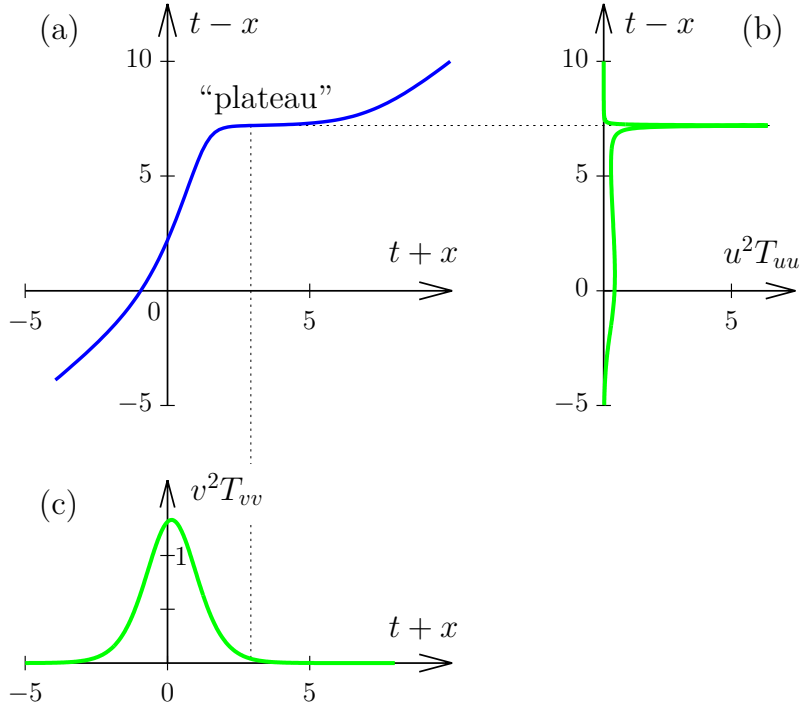


Figure 9. Solution (3.15) at almost critical values of parameters $s = b = e^{-2\phi_0} = 1$ and $a = a_{cr} - 10^{-3}$, where $a_{cr} = -1/\sqrt{3}$ and we use $\lambda = 1$ units. In this case $C \approx 7 \times 10^{-4} \ll 1$. Figure (a) shows the boundary $u = U(v)$ in the asymptotically flat light-cone coordinates $t+x = \log(\lambda v)/\lambda$, $t-x = -\log(-\lambda u)/\lambda$, see Eq. (2.11). In Figs. (b), (c) we plot the outgoing and incoming energy fluxes $u^2 T_{uu}$ and $v^2 T_{vv}$ as functions of $t-x$ and $t+x$, respectively.

Let us find the boundary $U(v)$ in the “plateau” region where v is large and $T_{vv}(v)$ is small. In this case Eq. (2.13) can be solved perturbatively by representing $\psi = 1 + \psi^{(1)} + \psi^{(2)} + \dots$, where $\psi^{(k)} \propto (T_{vv})^k$. Namely, using $\psi \approx 1$ in the r.h.s. of Eq. (2.13), we obtain,

$$\psi^{(1)}(v) = Cv + e^{2\phi_0} [g(v) - g_\infty] , \quad (4.1)$$

where the function $g(v)$ is introduced in Eq. (2.8) and g_∞ is its value at $v \rightarrow +\infty$. Note that the linear asymptotics $Cv \ll 1$ of the solution enters the first-order part (4.1) because in the near-critical regime $\partial_v \psi \approx C$ is small at large v . In what follows we will regard C as a parameter of the expansion. Using $\psi \approx 1 + \psi^{(1)}$ in the r.h.s. of Eq. (2.13), we get

$$\partial_v \psi^{(2)}(v) = e^{2\phi_0}(g - g_\infty) (e^{2\phi_0} \partial_v g - C) + e^{2\phi_0} C v \partial_v g + e^{4\phi_0} \int_v^\infty dv' (\partial_{v'} g)^2 .$$

The higher-order corrections $\psi^{(n)}$ are obtained in similar way.

Now, we compute the reflected energy flux $T_{uu}(u)$ and the boundary function $U(v)$ using Eqs. (2.14) and (2.12), respectively,

$$T_{uu}(U(v)) \approx \frac{\lambda^4 e^{4\phi_0} T_{vv}(v)}{[C + e^{2\phi_0} g_v(v)]^4} , \quad (4.2)$$

$$\lambda^2 U(v) \approx -e^{-2\phi_0} C + e^{-2\phi_0} C^2 v + 2C(g - g_\infty) - e^{2\phi_0} \int_v^\infty dv' (\partial_{v'} g)^2 . \quad (4.3)$$

We kept one and two orders of the expansion in Eqs. (4.2) and (4.3), respectively. Note that the leading (first) term in $U(v)$ is constant; this behavior corresponds to the “plateau” in Fig. 9a. At the same time, the reflected flux (4.2) has a peak at large v corresponding to $\partial_v g \sim C e^{-2\phi_0}$. This peak is narrow in terms of slowly-changing $u = U(v)$ in accordance with Fig. 9b.

Using the soliton asymptotics $T_{vv} \propto v^{-4}$ and $\partial_v g \propto v^{-3}$, one finds that the peak in Eq. (4.2) occurs at $v \propto C^{-1/3}$, and its width Δv is of the same order. The respective value of $U(v)$ is approximately given by the first term in Eq. (4.3), while the width of the peak $\Delta U \propto C^{2/3} U$ is controlled by the second-order terms. In the critical limit $C \rightarrow 0$ the peak of $T_{uu}(u)$ is infinitely high and narrow.

Calculating the total energy within the “thunderpop” at $C \rightarrow 0$, we obtain,

$$E_{\text{peak}} = \lambda \int_{u \sim C} |u| du T_{uu}(u) \rightarrow -2\lambda C \int_0^{+\infty} \frac{dv \partial_v^2 g(v)}{[C + e^{2\phi_0} \partial_v g(v)]^2} \rightarrow 2\lambda e^{-2\phi_0}$$

where Eqs. (4.2), (4.3) were used. The value of E_{peak} coincides with the minimal black hole mass M_{cr} implying that the peak of $T_{uu}(u)$ tends to a δ -function in the critical limit.

4.2 Thunderpop instability

Since our model is equipped with the general solution, one can assume that it is integrable, i.e. has a complete set of conserved quantities $\{I_k\}$ smoothly foliating the phase space. In the in-sector these quantities are arbitrary functionals $I_k[f_{in}]$ of conserved $f_{in}(v)$, cf. [57]. Then, I_k can be computed at arbitrary space-like line:

one evolves the Cauchy data at this line back in time, extracts the incoming wave¹⁴ $f_{in}(v)$, and calculates $I_k[f_{in}]$. The quantities $\{I_k\}$ obtained in this way are conserved by definition. For example, considering the out-sector, one gets $I_k[f_{out}] \equiv I_k[f_{in}]$ if $f_{out}(u)$ and $f_{in}(v)$ are related by classical evolution, Eq. (2.9).

Let us argue, however, that $\{I_k\}$ cannot be smoothly defined in the near-critical regime because the map $f_{in} \rightarrow f_{out}$ in this case is essentially singular.

To simplify the argument, we consider solutions with the modulated flux at large v ,

$$T_{vv} = (\partial_v f_{in})^2, \quad \partial_v f_{in} \approx A v^{-2} \cos(\omega \ln(\lambda v)) \quad \text{at} \quad v \gtrsim C^{-1/3}, \quad (4.4)$$

where C is the small parameter of the near-critical expansion. If ω is small as well, the asymptotics of T_{vv} is almost power-law, like in the ordinary solitons. However, the “thunderpop” part of the reflected flux represents squeezed and amplified tail of T_{vv} at $v \sim C^{-1/3}$, see Fig. 9. It should be essentially modulated. For simplicity, let us characterize the outgoing wave packet with a single quantity

$$\begin{aligned} \mathcal{I}_3(C, \omega) &\equiv \int_{-\infty}^{+\infty} d(t-x) (\partial_{t-x} f_{out})^3 = \Delta \mathcal{I}_3(C, \omega) + \text{const}, \\ \Delta \mathcal{I}_3 &= \int_0^{\infty} dv \frac{C^2 (\partial_v f_{in})^3}{[C + e^{2\phi_0} g_v(v)]^4}, \end{aligned} \quad (4.5)$$

where we used the flat coordinates (2.11) in the definition of \mathcal{I}_3 , then separated the “thunderpop” part $\Delta \mathcal{I}_3$ of the integral at $t-x = -\log(-\lambda u)/\lambda \gtrsim \log C$ from the (C, ω) -independent contribution at smaller $t-x$. In the second line we substituted the “thunderpop” profile (4.2), (4.3) and extended the integration range to $v \geq 0$. Now, one substitutes the asymptotics (4.4) into Eq. (4.5) and finds that $\Delta \mathcal{I}_3(C, \omega)$ is quasi-periodic. Indeed, change of the integration variable $v \mapsto v e^{2\pi n/\omega}$ with integer n gives relation¹⁵ $\Delta \mathcal{I}_3(e^{6\pi n/\omega} C, \omega) = e^{-2\pi n/\omega} \Delta \mathcal{I}_3(C, \omega)$. Thus, $\Delta \mathcal{I}_3 = C^{-1/3} \mathcal{J}(\omega \log C)$, where $\mathcal{J}(x)$ is 6π -periodic.

We see that $\Delta \mathcal{I}_3$ has an essential singularity at $\omega = C = 0$. Indeed, taking the limit $C \rightarrow 0$ along the paths $\omega \log C = \text{const}$, one obtains $\Delta \mathcal{I}_3 \rightarrow -\infty, 0$, or $+\infty$, see Fig. 10. Thus, any value of $\Delta \mathcal{I}_3$ can be obtained by adjusting the limiting path.

The above property ascertains dynamical chaos in the critical limit of our model. Indeed, infinitesimally small changes (4.4) of the initial data at small C produce outgoing fluxes with essentially different values of \mathcal{I}_3 . This prevents one from characterizing the critical evolution with a set of smooth conserved quantities I_k . Indeed, all functionals $I_k[f_{in}]$, being smooth in the in-sector, are not sensitive to ω at small

¹⁴Recall that all our solutions start from flat space-time in the infinite past.

¹⁵In this case $g'(v e^{2\pi n/\omega}) = e^{-6\pi n/\omega} g'(v)$, where the derivative is taken with respect to the argument, see Eqs. (2.8).

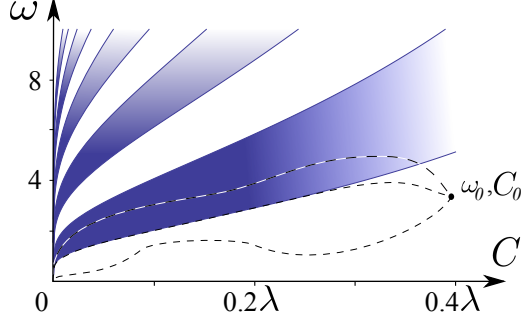


Figure 10. Regions $\Delta\mathcal{I}_3 > 0$ (white) and $\Delta\mathcal{I}_3 < 0$ (blue) in the (C, ω) plane. We use the solution (4.4) with $A^2 = 12e^{-2\phi_0}/\lambda^2$.

values of latter. Thus, they fail to describe essentially different out-states $f_{out}(u)$ at different ω . From a more general perspective, one can introduce the integrals which are smooth either in the in-sector or in the out-sector, but not in both.

5 Discussion

In this paper we considered two-dimensional CGHS model with a regulating dynamical boundary [33, 34]. This model is weakly coupled and causally similar to the spherically-symmetric gravity in many dimensions. We demonstrated that the classical field equations in this model are exactly solvable. We constructed their general solution and studied in detail a large subset of soliton solutions with transparent properties. We illustrated the results with many explicit examples hoping that this model may serve as a practical playground for black hole physics.

In the critical regime i.e. at the verge of black hole formation, the dynamics of our model displays instabilities specific to chaotic systems. This feature is similar to the near-horizon chaos studied recently in the context of AdS/CFT correspondence [21–26]. We argued that it hinders global integrability of the model.

We see several applications of our results. First, solvability may be extended to the one-loop semiclassical level once a reflective boundary is added to the RST model [5]. This approach, if successful, will produce exact solutions describing black hole formation and evaporation. The singularities of such solutions should be either covered by the boundary or hidden behind the space-like line $\phi = \phi_0$, see Fig. 4b. Then a complete Penrose diagram for the evaporation process may be obtained, cf. [38, 40, 41, 45].

Second, in the alternative approach one may directly add one-loop corrections to the classical equations in our model and integrate the resulting system numerically, cf. [58, 59]. By the same reasons as above, the respective solutions should completely describe the process of black hole evaporation.

Third and finally, the model of this paper is ideal for applying the semiclassical method of [60] which relates calculation of the exponentially suppressed S -matrix elements to certain complex classical solutions. The results of such calculations may be used to test unitarity of the gravitational S -matrix [60].

Acknowledgments. We thank S. Sibiryakov for participating at early stages of this project. We are grateful to École Polytechnique Fédérale de Lausanne for hospitality during our visits. This work was supported by the grant RSCF 14-22-00161.

A Field equations and boundary conditions

A.1 Derivation

Field equations in the bulk are obtained by varying the action (2.1) with respect to $g_{\mu\nu}$, ϕ , and f , and ignoring the boundary terms,

$$4e^{-2\phi}\nabla_\mu\nabla_\nu\phi + 4g_{\mu\nu}e^{-2\phi}[(\nabla\phi)^2 - \nabla^2\phi - \lambda^2] = \nabla_\mu f\nabla_\nu f - \frac{1}{2}g_{\mu\nu}(\nabla f)^2, \quad (\text{A.1})$$

$$(\nabla\phi)^2 - \nabla^2\phi - \lambda^2 = R/4, \quad (\text{A.2})$$

$$\nabla^2 f = 0. \quad (\text{A.3})$$

The first line here relates the energy-momentum tensors of ϕ and f , $-T_{\mu\nu}^{(\Phi)} = T_{\mu\nu}^{(f)}$. The second line implies, in addition, that the rescaled metric $e^{-2\phi}g_{\mu\nu}$ is flat.

To find the boundary conditions at the line $\phi = \phi_0$, we keep the boundary terms in the variation of the action. For a start, let us consider variations preserving the coordinate position of the boundary $\phi = \phi_0$. We take $\delta\phi = 0$ at this line and fix the direction of its outer normal, $\delta n_\mu \propto n_\mu$. The integration domains in Eq. (2.1) are unchanged by such variations. One obtains,

$$\delta S = - \int_{\phi=\phi_0} d\tau [2h^{\mu\nu}\delta h_{\mu\nu}e^{-2\phi_0}(n^\kappa\nabla_\kappa\phi - \lambda) + \delta f n^\kappa\nabla_\kappa f] = 0, \quad (\text{A.4})$$

where we canceled the bulk terms using Eqs. (A.1)—(A.3) and introduced the induced metric $h_{\mu\nu} \equiv g_{\mu\nu} - n_\mu n_\nu$. The variation (A.4) gives the boundary conditions (2.2). Note that the space-time is flat near the boundary: one obtains $R = 0$ at $\phi = \phi_0$ using the first of Eqs. (2.2), Eq. (A.2) and the trace of Eq. (A.1).

Now, let us consider general variations shifting the position of the boundary. They are combinations of the general coordinate transformations and position-preserving variations considered above. The action is unchanged by these variations because it is covariant and already extremized at fixed coordinate position of the boundary.

A.2 Solution in the conformal gauge

Let us review the exact solution [4] of the bulk equations (A.1)—(A.3), see [1, 2] for details.

In the light-cone frame (2.4) Eq. (A.3) takes the form $\partial_u \partial_v f = 0$, its general solution is given by Eq. (2.5). Combining Eq. (A.2) with the trace of Eq. (A.1) and substituting $R = 8e^{-2\rho} \partial_u \partial_v \rho$, we obtain,

$$\partial_u \partial_v (\phi - \rho) = 0 \quad \Rightarrow \quad \phi = \rho ,$$

where the residual coordinate freedom¹⁶ was fixed in the last equation. After that Eqs. (A.1), namely,

$$\begin{aligned} \partial_u^2 e^{-2\phi} &= -\frac{1}{2} (\partial_u f)^2 , \\ \partial_v^2 e^{-2\phi} &= -\frac{1}{2} (\partial_v f)^2 , \\ \partial_u \partial_v e^{-2\phi} &= -\lambda^2 , \end{aligned}$$

are integrated into

$$e^{-2\rho} = e^{-2\phi} = \frac{M_-}{2\lambda} - \lambda^2 (u - u_0)(v - v_0) + g(v) + h(u) . \quad (\text{A.5})$$

In this expression M_- , u_0 , and v_0 are the integration constants, while the functions $g(v)$ and $h(u)$ were introduced in Eq. (2.8). We fix $u_0 = v_0 = 0$ by shifting u and v . After that, M_- represents the mass of the white hole in the infinite past [1, 2]. Indeed, the past time infinity i^- is reached at $u \rightarrow -\infty$, $v \rightarrow 0$, and constant ϕ , cf. Eq. (2.3). If $M_- \neq 0$, the curvature remains nonzero in this limit,

$$R = 4e^{2\rho} (\partial_u e^{-2\rho}) (\partial_v e^{-2\rho}) - 4\partial_u \partial_v e^{-2\rho} \rightarrow 2\lambda e^{2\phi} M_- ,$$

where Eq. (A.5) with $u_0 = v_0 = 0$ was used. In this paper we consider solutions starting from flat space-time. Thus, $M_- = 0$, and Eq. (A.5) turns into Eq. (2.7).

It is worth noting that the patch $u \in (-\infty, 0)$ and $v \in (0, +\infty)$ covers all space-time accessible to the outside observer. Indeed, the past and future time infinities i^\pm in Fig. 1b are reached in the limits $u \rightarrow -\infty$ and $v \rightarrow +\infty$ at finite values of the dilaton field ϕ . By Eq. (2.7), the product uv remains finite in these limits implying $v \rightarrow +0$ as $u \rightarrow -\infty$ and $u \rightarrow -0$ as $v \rightarrow +\infty$.

We proceed by deriving equation of motion for the boundary $u = U(v)$ satisfying $\phi(U(v), v) = \phi_0$. Taking derivative of Eq. (2.7) along this line, we find,

$$0 = \frac{d}{dv} e^{-2\phi_0} = U' [\partial_u h - \lambda^2 v] + \partial_v g - \lambda^2 U , \quad \text{at} \quad u = U(v) , \quad (\text{A.6})$$

¹⁶Namely, the transformations $u \rightarrow \tilde{u}(u)$, $v \rightarrow \tilde{v}(v)$ preserving the metric (2.4).

where $U' \equiv dU/dv > 0$ because the boundary is time-like. The other two equations come from the boundary conditions (2.2). Introducing the unit outer normal

$$n^u = e^{-\phi_0} \sqrt{U'} , \quad n^v = -e^{-\phi_0} / \sqrt{U'}$$

and using Eq. (A.6), we rewrite Eqs. (2.2) as equation of motion for the boundary and reflection law for the matter field, Eqs. (2.9).

At this point, we have three equations, Eqs. (A.6) and (2.9), for the two unknown functions $f_{out}(u)$ and $U(v)$. Note, however, that Eq. (A.6) follows from the other two equations. Indeed,

$$\frac{d}{dv} \left(\frac{\partial_v g - \lambda^2 U}{U'} \right) = \lambda^2 e^{-2\varphi_0} \frac{d}{dv} (\partial_v g - \lambda^2 U)^{-1} = \frac{(\partial_v f_{in})^2 / 2 + \lambda^2 U'}{U'} = \frac{d}{dv} (\lambda^2 v - \partial_u h) ,$$

where we expressed U' and g via Eqs. (2.9) and (2.8) in the first and second equalities, then turned $f_{in} \rightarrow f_{out}$ by the second of Eqs. (2.9) and used the equation for U' again. One concludes that Eq. (A.6) is automatically satisfied once the initial conditions for $U(v)$ are chosen correctly.

B Bethe Ansatz for the Gaudin model

In this Appendix we review Bethe Ansatz solution of the Gaudin model (3.16), see [46–48] for details.

One introduces raising and lowering operators $\hat{s}^\pm(v) = \hat{s}^1(v) \pm i\hat{s}^2(v)$ for the position-dependent spin (3.17). The commutation rules of these operators are

$$[\hat{s}^-(v), \hat{s}^+(w)] = 2 \frac{\hat{s}^3(v) - \hat{s}^3(w)}{v - w} , \quad [\hat{s}^3(v), \hat{s}^\pm(w)] = \mp \frac{\hat{s}^\pm(v) - \hat{s}^\pm(w)}{v - w} .$$

The Hamiltonian $\hat{\mathcal{T}}(v)$ takes the form

$$\hat{\mathcal{T}}(v) = \frac{1}{2} \hat{s}^+(v) \hat{s}^-(v) + \frac{1}{2} \hat{s}^-(v) \hat{s}^+(v) + (\hat{s}^3(v))^2 . \quad (\text{B.1})$$

Now, it is straightforward to check that the spin-down state (3.18) is an eigenstate:

$$\hat{\mathcal{T}}(v)|0\rangle = [(W_0)^2 + \partial_v W_0] |0\rangle , \quad \text{where} \quad W_0(v) = - \sum_n \frac{s_n}{v - v_n}$$

is the eigenvalue of the third spin component, $\hat{s}^3(v)|0\rangle = W_0(v)|0\rangle$.

One explicitly acts with $\hat{\mathcal{T}}(v)$, Eq. (B.1), on the state (3.19) and obtains,

$$\hat{\mathcal{T}}(v)|\tilde{v}_1, \dots, \tilde{v}_M\rangle = \mathcal{T}(v)|\tilde{v}_1, \dots, \tilde{v}_M\rangle - \sum_{m=1}^M \frac{2L_m}{v - \tilde{v}_m} |\tilde{v}_1, \dots, \tilde{v}_m \mapsto v, \dots, \tilde{v}_M\rangle , \quad (\text{B.2})$$

where $\mathcal{T}(v)$ is given by Eq. (3.21), L_m is the left-hand side of Eq. (3.20), and arrow denotes substitution. Note that the relations

$$[\hat{\mathcal{T}}(v), \hat{s}^+(w)] = \frac{2}{v-w} (\hat{s}^+(w)\hat{s}^3(v) - \hat{s}^+(v)\hat{s}^3(w)) ,$$

$$\hat{s}^3(v)|\tilde{v}_1, \dots, \tilde{v}_M\rangle = W(v)|\tilde{v}_1, \dots, \tilde{v}_M\rangle - \sum_m \frac{1}{v - \tilde{v}_m} |\tilde{v}_1, \dots, \tilde{v}_m \rightarrow v, \dots, \tilde{v}_M\rangle ,$$

where $W(v)$ is defined in Eq. (3.21), are helpful for deriving Eq. (B.2).

We conclude that Eq. (B.2) coincides with the eigenproblem for $\hat{\mathcal{T}}(v)$ if the Bethe equations $L_m = 0$, Eqs. (3.20), are satisfied. In this case the Bethe states (3.19) are eigenstates of the Gaudin Hamiltonians (3.16). Moreover, one can prove [46–48] that the basis (3.19) is complete.

References

- [1] S. B. Giddings, *Quantum mechanics of black holes*, [hep-th/9412138](#).
- [2] A. Strominger, *Les Houches lectures on black holes*, [hep-th/9501071](#).
- [3] D. Grumiller, W. Kummer and D. V. Vassilevich, *Dilaton gravity in two-dimensions*, Phys. Rept. **369** (2002) 327 [[hep-th/0204253](#)].
- [4] C. G. Callan, Jr., S. B. Giddings, J. A. Harvey and A. Strominger, *Evanescent black holes*, Phys. Rev. D **45** (1992) R1005 [[hep-th/9111056](#)].
- [5] J. G. Russo, L. Susskind and L. Thorlacius, *The Endpoint of Hawking radiation*, Phys. Rev. D **46** (1992) 3444 [[hep-th/9206070](#)].
- [6] S. B. Giddings, *The gravitational S-matrix: Erice lectures*, Subnucl. Ser. **48** (2013) 93 [[arXiv:1105.2036](#)].
- [7] G. 't Hooft, *The Scattering matrix approach for the quantum black hole: An Overview*, Int. J. Mod. Phys. A **11** (1996) 4623 [[gr-qc/9607022](#)].
- [8] G. Dvali, C. Gomez, R. S. Isermann, D. Lüst and S. Stieberger, *Black hole formation and classicalization in ultra-Planckian $2 \rightarrow N$ scattering*, Nucl. Phys. B **893** (2015) 187 [[arXiv:1409.7405](#)].
- [9] S. W. Hawking, *Particle Creation by Black Holes*, Commun. Math. Phys. **43** (1975) 199 [*Erratum-ibid* **46** (1976) 206].
- [10] S. W. Hawking, *Breakdown of Predictability in Gravitational Collapse*, Phys. Rev. D **14** (1976) 2460.
- [11] J. M. Maldacena, *The Large N limit of superconformal field theories and supergravity*, Int. J. Theor. Phys. **38** (1999) 1113 [Adv. Theor. Math. Phys. **2** (1998) 231] [[hep-th/9711200](#)].
- [12] J. M. Maldacena, *Eternal black holes in anti-de Sitter*, JHEP **0304** (2003) 021 [[hep-th/0106112](#)].

- [13] A. Almheiri, D. Marolf, J. Polchinski and J. Sully, *Black Holes: Complementarity or Firewalls?*, JHEP **1302** (2013) 062 [[arXiv:1207.3123](#)].
- [14] A. Almheiri, D. Marolf, J. Polchinski, D. Stanford and J. Sully, *An Apologia for Firewalls*, JHEP **1309** (2013) 018 [[arXiv:1304.6483](#)].
- [15] S. L. Braunstein, S. Pirandola and K. Życzkowski, *Better Late than Never: Information Retrieval from Black Holes*, Phys. Rev. Lett. **110** (2013) 101301 [[arXiv:0907.1190](#)].
- [16] S. D. Mathur, *The Information paradox: A Pedagogical introduction*, Class. Quant. Grav. **26** (2009) 224001 [[arXiv:0909.1038](#)].
- [17] V. Cardoso, E. Franzin and P. Pani, *Is the gravitational-wave ringdown a probe of the event horizon?*, Phys. Rev. Lett. **116** (2016) 171101 [*Erratum-ibid* **117** (2016) 089902] [[arXiv:1602.07309](#)].
- [18] V. Cardoso, S. Hopper, C. F. B. Macedo, C. Palenzuela and P. Pani, *Gravitational-wave signatures of exotic compact objects and of quantum corrections at the horizon scale*, Phys. Rev. D **94** (2016) 084031 [[arXiv:1608.08637](#)].
- [19] B. P. Abbott *et al.* [LIGO Scientific and Virgo Collaborations], *Observation of Gravitational Waves from a Binary Black Hole Merger*, Phys. Rev. Lett. **116** (2016) 061102 [[arXiv:1602.03837](#)].
- [20] J. Abedi, H. Dykaar and N. Afshordi, *Echoes from the Abyss: Evidence for Planck-scale structure at black hole horizons*, [arXiv:1612.00266](#).
- [21] S. H. Shenker and D. Stanford, *Black holes and the butterfly effect*, JHEP **1403** (2014) 067 [[arXiv:1306.0622](#)].
- [22] S. H. Shenker and D. Stanford, *Stringy effects in scrambling*, JHEP **1505** (2015) 132 [[arXiv:1412.6087](#)].
- [23] J. Polchinski, *Chaos in the black hole S-matrix*, [arXiv:1505.08108](#).
- [24] J. Maldacena, S. H. Shenker and D. Stanford, *A bound on chaos*, JHEP **1608** (2016) 106 [[arXiv:1503.01409](#)].
- [25] G. Turiaci and H. Verlinde, *On CFT and Quantum Chaos*, JHEP **1612** (2016) 110 [[arXiv:1603.03020](#)].
- [26] K. Hashimoto and N. Tanahashi, *Universality in Chaos of Particle Motion near Black Hole Horizon*, Phys. Rev. D **95** (2017) 024007 [[arXiv:1610.06070](#)].
- [27] E. T. Akhmedov, H. Godazgar and F. K. Popov, *Hawking radiation and secularly growing loop corrections*, Phys. Rev. D **93** (2016) 024029 [[arXiv:1508.07500](#)].
- [28] S. W. Hawking, M. J. Perry and A. Strominger, *Soft Hair on Black Holes*, Phys. Rev. Lett. **116** (2016) 231301 [[arXiv:1601.00921](#)].
- [29] M. Mirbabayi and M. Porrati, *Dressed Hard States and Black Hole Soft Hair*, Phys. Rev. Lett. **117** (2016) 211301 [[arXiv:1607.03120](#)].

- [30] A. Ashtekar, V. Taveras and M. Varadarajan, *Information is Not Lost in the Evaporation of 2-dimensional Black Holes*, Phys. Rev. Lett. **100** (2008) 211302 [[arXiv:0801.1811](#)].
- [31] S. R. Das and S. Mukherji, *Boundary dynamics in dilaton gravity*, Mod. Phys. Lett. A **9** (1994) 3105 [[hep-th/9407015](#)].
- [32] A. Almheiri and J. Sully, *An Uneventful Horizon in Two Dimensions*, JHEP **1402** (2014) 108 [[arXiv:1307.8149](#)].
- [33] T.-D. Chung and H. L. Verlinde, *Dynamical moving mirrors and black holes*, Nucl. Phys. B **418** (1994) 305 [[hep-th/9311007](#)].
- [34] K. Schoutens, H. L. Verlinde and E. P. Verlinde, *Black hole evaporation and quantum gravity*, In *Berkeley 1993, Proceedings, Strings '93* 22, and In *Trieste 1993, Proceedings, String theory, gauge theory and quantum gravity '93* 1, [[hep-th/9401081](#)].
- [35] A. Almheiri and J. Polchinski, *Models of AdS_2 backreaction and holography*, JHEP **1511** (2015) 014 [[arXiv:1402.6334](#)].
- [36] J. Maldacena, D. Stanford and Z. Yang, *Conformal symmetry and its breaking in two dimensional Nearly Anti-de-Sitter space*, PTEP **2016** (2016) 12C104 [[arXiv:1606.01857](#)].
- [37] J. Engelsöy, T. G. Mertens and H. Verlinde, *An investigation of AdS_2 backreaction and holography*, JHEP **1607** (2016) 139 [[arXiv:1606.03438](#)].
- [38] S. R. Das and S. Mukherji, *Black hole formation and space-time fluctuations in two-dimensional dilaton gravity and complementarity*, Phys. Rev. D **50** (1994) 930 [[hep-th/9401102](#)].
- [39] A. Strominger and L. Thorlacius, *Conformally invariant boundary conditions for dilaton gravity*, Phys. Rev. D **50** (1994) 5177 [[hep-th/9405084](#)].
- [40] S. Bose, L. Parker and Y. Peleg, *Hawking radiation and unitary evolution*, Phys. Rev. Lett. **76** (1996) 861 [[gr-qc/9508027](#)].
- [41] S. Bose, L. Parker and Y. Peleg, *Predictability and semiclassical approximation at the onset of black hole formation*, Phys. Rev. D **54** (1996) 7490 [[hep-th/9606152](#)].
- [42] J. G. Russo, L. Susskind and L. Thorlacius, *Cosmic censorship in two-dimensional gravity*, Phys. Rev. D **47** (1993) 533 [[hep-th/9209012](#)].
- [43] E. P. Verlinde and H. L. Verlinde, *A quantum S-matrix for two-dimensional black hole formation and evaporation*, Nucl. Phys. B **406** (1993) 43 [[hep-th/9302022](#)].
- [44] K. Schoutens, H. L. Verlinde and E. P. Verlinde, *Quantum black hole evaporation*, Phys. Rev. D **48** (1993) 2670 [[hep-th/9304128](#)].
- [45] Y. Peleg, S. Bose and L. Parker, *Choptuik scaling and quantum effects in 2-d dilaton gravity*, Phys. Rev. D **55** (1997) 4525 [[gr-qc/9608040](#)].

- [46] M. Gaudin, *Diagonalization d'une classe d'hamiltoniens de spin*, J. Physique **37** (1976) 1087.
- [47] B. Feigin, E. Frenkel and N. Reshetikhin, *Gaudin model, Bethe ansatz and correlation functions at the critical level*, Commun. Math. Phys. **166** (1994) 27 [[hep-th/9402022](#)].
- [48] E. Frenkel, *Affine algebras, Langlands duality and Bethe ansatz*, [q-alg/9506003](#).
- [49] E. Poisson, *A Relativist's Toolkit. The Mathematics of Black-Hole Mechanics*, Cambridge University Press, 2004.
- [50] J. Teschner, *Quantization of the Hitchin moduli spaces, Liouville theory, and the geometric Langlands correspondence I*, Adv. Theor. Math. Phys. **15** (2011) 471 [[arXiv:1005.2846](#)].
- [51] P. Di Francesco, P. Mathieu and D. Sénéchal, *Conformal Field Theory*, Springer-Verlag New York, 1997.
- [52] S. Y. Vernov, *Construction of solutions for the generalized Henon-Heiles system with the help of the Painleve test*, Theor. Math. Phys. **135** (2003) 792 [[math-ph/0209063](#)].
- [53] S. J. van Tongeren, *Introduction to the thermodynamic Bethe ansatz*, J. Phys. A **49** (2016) 323005 [[arXiv:1606.02951](#)].
- [54] Y. Kiem and D. Park, *Static and Dynamic Analysis of a Massless Scalar Field Coupled with a Class of Gravity Theories*, Phys. Rev. D **53** (1996) 747 [[arXiv:hep-th/9504021](#)].
- [55] M. W. Choptuik, *Universality and scaling in gravitational collapse of a massless scalar field*, Phys. Rev. Lett. **70** (1993) 9.
- [56] C. Gundlach, *Critical phenomena in gravitational collapse*, Phys. Rept. **376** (2003) 339 [[gr-qc/0210101](#)].
- [57] V. V. Bazhanov, S. L. Lukyanov and A. B. Zamolodchikov, *Integrable structure of conformal field theory, quantum KdV theory and thermodynamic Bethe ansatz*, Commun. Math. Phys. **177** (1996) 381 [[hep-th/9412229](#)].
- [58] A. Ashtekar, F. Pretorius and F. M. Ramazanoglu, *Surprises in the Evaporation of 2-Dimensional Black Holes*, Phys. Rev. Lett. **106** (2011) 161303 [[arXiv:1011.6442](#)].
- [59] A. Ashtekar, F. Pretorius and F. M. Ramazanoglu, *Evaporation of 2-Dimensional Black Holes*, Phys. Rev. D **83** (2011) 044040 [[arXiv:1012.0077](#)].
- [60] F. Bezrukov, D. Levkov and S. Sibiryakov, *Semiclassical S-matrix for black holes*, JHEP **1512** (2015) 002 [[arXiv:1503.07181](#)].